

Epithelial V-like Antigen (EVA), a Novel Member of the Immunoglobulin Superfamily, Expressed in Embryonic Epithelia with a Potential Role as Homotypic Adhesion Molecule in Thymus Histogenesis

Maria Guttinger,* Francesca Sutti,* Maddalena Panigada,* Simona Porcellini,* Barbara Merati,* Margherita Mariani,* Tabet Teesalu,* G. Giacomo Consalez,* and Fabio Grassi[‡]

*Department of Biological and Technological Research (DIBIT), San Raffaele Scientific Institute (HSR); and[‡]Dipartimento di Biologia e Genetica per le Scienze Mediche, Università di Milano at DIBIT-HSR, I-20132 Milan, Italy

Abstract. Thymus development depends on a complex series of interactions between thymocytes and the stromal component of the organ. To identify regulated genes during this codependent developmental relationship, we have applied an RNA fingerprinting technique to the analysis of thymus expansion and maturation induced in recombinase-deficient mice injected with anti-CD3 antibodies. This approach led us to the identification of a gene encoding a new member of the immunoglobulin superfamily, named epithelial V-like antigen (EVA), which is expressed in thymus epithelium and

strongly downregulated by thymocyte developmental progression. This gene is expressed in the thymus and in several epithelial structures early in embryogenesis. EVA is highly homologous to the myelin protein zero and, in thymus-derived epithelial cell lines, is poorly soluble in nonionic detergents, strongly suggesting an association to the cytoskeleton. Its capacity to mediate cell adhesion through a homophilic interaction and its selective regulation by T cell maturation might imply the participation of EVA in the earliest phases of thymus organogenesis.

THYMUS organogenesis depends upon a complex series of interactions among cells of different embryonic origin. The lymphoid epithelial thymic primordium originates from the third pharyngeal pouch and requires the inductive effect of mesenchyme for appropriate morphogenesis (Auerbach, 1960). Subsequently, the advent of hemopoietic precursors at day 10.5 of fetal life initiates the multiple thymocyte–stroma interactions that critically settle the architectural and functional organization of the mature organ (van Ewijk, 1991; Boyd et al., 1993).

The potential role of various cell adhesion molecules in governing early stages of thymocyte development, as well as thymic epithelium organization, has been described. LFA-1/ICAM-1 interactions have been shown to play a role in thymocyte maturation and proliferation (Fine and Kruisbeek, 1991). Thy-1 supports adhesion of thymocyte to thymic epithelial cells through a heterophilic interaction that can be inhibited by sulfated glycans (Hueber et al., 1992). The $\alpha\beta 4$ (Wadsworth et al., 1992) and VLA-4 (Sawada et al., 1992) integrins display a developmentally regulated pattern of expression with the highest level in

thymocyte before TCR rearrangement, suggesting a role for these molecules in mediating adhesion of early thymocyte to stroma. Extracellular matrix proteins have been detected in the thymus; it has been shown that early thymocytes adhere to thymus epithelium through fibronectin expressed by the stromal cell and that blockade of this interaction has an impact on T cell maturation (Utsumi et al., 1991). Additionally, merosin–thymocyte interaction has been suggested to play a role in T cell development (Chang et al., 1993). Recently, homophilic E-cadherin interactions have been shown to be critically involved in the generation of a functional thymic environment and in cellular interactions occurring in the early phases of T cell development (Muller et al., 1997).

Maturation of $\alpha\beta$ T cells is characterized by the progression of double negative (DN)¹ precursors expressing neither CD4 nor CD8, to a double positive (DP) CD4⁺8⁺ stage after low-level CD8 expression. As defined by interleukin-2 (IL-2) receptor (CD25) and CD44 expression, the DN stage can be ordered in the following developmental

T. Teesalu's present address is Department of Virology, Haartman Institute, University of Helsinki, 00014 Helsinki, Finland.

Address all correspondence to Maria Guttinger, DIBIT-HSR, via Olgettina 58, I-20132 Milan, Italy. Tel.: (39) 226-434-797. Fax: (39) 226-434-786. E-mail: guttinger.maria@hsr.it (note change)

1. *Abbreviations used in this paper:* aa, amino acid; DN, double negative; DP, double positive; endo-H, endo- β -N-acetylglucosaminidase H; EST, expressed sequence tag; *Eva*, epithelial V-like antigen; KRH, Krebs-Ringer-Hepes; p.c., post coitum; Po, myelin protein zero; RAG-2^{-/-}, recombinase-activating-2 gene deficient; RPA, RNase protection assay; RT, reverse transcriptase.

sequence of phenotypes: DN CD44⁺25⁻ > DN CD44⁺25⁺ > DN CD44⁻25⁺ (Godfrey and Zlotnik, 1993). The attainment of DP stage is defined β selection, because it is mainly controlled by TCR β gene rearrangement and expression in association with pre-TCR- α (von Boehmer and Fehling, 1997). Cells that have succeeded in β selection expand and undergo a further recombination event allowing TCR- α rearrangements to occur (Petrie et al., 1993), followed by major histocompatibility complex-driven clonotypic $\alpha\beta$ selection (von Boehmer, 1994). Recombinase-activating-2 gene deficient (RAG-2^{-/-}) mice, in which TCR- β gene cannot rearrange, display a block at the CD44⁻CD25⁺ stage (Shinkai et al., 1992). A scarcely populated cortex is apparent and there is absence of the medullary compartment (Holländer et al., 1995), consistent with the observed requirement for a functionally "mature" TCR-CD3 complex for the development of the medulla (Negishi et al., 1995). In vivo treatment of RAG-2^{-/-} mice with anti-CD3 ϵ mAb induces transition of DN into DP thymocytes with cell proliferation, cell size reduction, and other phenotypic modifications characteristic of this transition (Jacobs et al., 1994; Shinkai and Alt, 1994). In this respect, the RAG-deficient thymus offers a unique opportunity to obtain the earliest lymphoid precursors uncontaminated with later-stage cells, and an organ phenotypically arrested at 14 or 15 d of embryonic life that can be induced to expand and differentiate.

To identify genes whose expression is selectively regulated during thymus development, we applied a PCR-based differential screening approach (RNA fingerprinting) (Malgaretti et al., 1997), comparing thymus RNAs extracted from untreated RAG-2^{-/-} mice and from the same mutants treated in vivo with anti-CD3 ϵ antibodies. Among other genes displaying differential expression identified in this way, we have isolated a new member of the immunoglobulin gene superfamily. The gene, named epithelial V-like antigen (*Eva*), encodes a putative transmembrane type 1 glycoprotein, bearing an immunoglobulin V-type domain. The gene is expressed at high levels in the thymic epithelium of RAG-2^{-/-} mice and is almost completely downregulated by in vivo treatment with anti-CD3 ϵ mAbs. The gene is expressed in thymus-derived epithelial cell lines and in various epithelia in development and adulthood. Here, we present the cloning, sequence, and initial genetic, biochemical, and functional characterization of this new protein of potential relevance as homotypic adhesion molecule in development, specifically in the early stages of thymus organogenesis.

Materials and Methods

General Procedures

Standard molecular techniques, including nucleic acid purification, restriction analysis, gel electrophoresis, cloning, subcloning, dideoxy-sequencing, probe radiolabeling, Northern and Southern analysis, and library screening were performed according to established protocols (Sambrook et al., 1989).

Animals

4-wk-old C57BL/6 and CD-1 mice were purchased from Charles River Laboratories (Calco, Italy) and RAG-2^{-/-} mice were purchased from Bomholtgard (Ry, Denmark). All mice were bred and maintained in a

specific pathogen-free facility at DIBIT-HSR Scientific Institute. RAG-2^{-/-} mice were i.v. injected with 50 μ g of anti-CD3 ϵ mAb.

Cell Lines, Antibodies, and Primers

The following cell lines were used in this study: thymus epithelium-derived A89A, A2T (Hiai et al., 1985), TEC (Glimcher et al., 1983), MTE (Lepesant et al., 1990), 24B6 (Yanagihara et al., 1981), and TNC.R3.1 (Nishimura et al., 1990); thymocyte-derived BW5147 (Hyman and Stallings, 1974), M15T, and M14T (Primi et al., 1988); thymic fibroblast 1D4 (Izon et al., 1994); NIH3T3 (CRL-1658; American Type Culture Collection, Rockville, MD); bone marrow stroma-derived BMS2 (Pietrangeli et al., 1988), M210 (provided by A. Aiuti, San Raffaele Scientific Institute, Milan, Italy), and MS-5 (Itoh et al., 1989); multipotent hemopoietic stem cell FDPC mix (Spooncer et al., 1986); fetal skin-derived dendritic cell FSDC (Girolomoni et al., 1995); macrophage cell line MT2 (Lutz et al., 1994); mature T cell line M15S (Primi et al., 1988); monkey COS7 fibroblasts (Gluzman, 1981); and CHO cells (provided by R. Sitia, San Raffaele Scientific Institute). All cell lines were maintained in DME (GIBCO BRL, Gaithersburg, MD) supplemented with 2 mM L-glutamine, 1 mM sodium pyruvate, 5 \times 10⁻⁵ M β -mercaptoethanol, 50 U/ml streptomycin, and 10% FCS.

The following mAbs were used in this study: 145-2C11 (anti-CD3 ϵ) (Leo et al., 1987); H129.19 (anti-CD4), 53-6.7 (anti-CD8), AMT-13 (anti-CD25), and AC-40 (anti-actin) (Sigma Chemical Co., St. Louis, MO); 9.3.4.HL.2 (anti-murine CD45) (TIB-122; American Type Culture Collection); G7 (anti-CD90/Thy-1), RA3-6B2 (anti-CD45R/B220) (PharMingen, San Diego, CA); F4/80 (anti-macrophage) (Austyn and Gordon, 1981); 9E10 (anti-myc, CRL-1279; American Type Culture Collection); 327 (anti-v-src) (Oncogene Science, Inc., Manhasset, NY). Rabbit antiserum specific for EVA was obtained by immunizing rabbit 833 with a peptide corresponding to the 21 NH₂-terminal residues of the predicted mature protein. The immune serum was affinity purified on EAH Sepharose 48 (Pharmacia Biotech, Inc., Piscataway, NJ) coupled to the relevant peptide. Rabbit complement was purchased from Cedarlane Labs, Ltd. (Hornby, Ontario, Canada).

The following primers were used in this study: DR122 5'-GGGACG-TCTACG; Eva forward G1.F 5'-CACGACTGGTGGCTCCGCT, G1.RT 5'-GGGTGGTCTGGGACGGAAAC; Eva reverse G1.A5 5'-GTGTG-CACAACGCTGAGCCGG, G1.T3ON 5'-GGGGTGTGATGGTGT-CCTC; β actin forward 5'-TGACGGGTCAACACACTGTGCC-ATCTA, β actin reverse 5'-CTAGAAGCATTTGCGGTGGACGATG-GAGG.

Gene Isolation and Sequence Analysis

PCR-based differential screening (RNA fingerprinting) (Welsh et al., 1995) was conducted as previously described (Corradi et al., 1996; Malgaretti et al., 1997) to compare mRNAs of thymi from untreated C57BL/6, RAG-2^{-/-} mice and RAG-2^{-/-} mice i.v. injected with 50 μ g of 145-2C11 mAb. In the case of treated animals, thymi were dissected 2, 6, and 48 h after antibody injection. DR122 was the arbitrary 12 mer primer used. Thymus RNA extracted from adult RAG-2^{-/-} mice was used to construct a cDNA library cloned into Lambda Zap II (Stratagene, La Jolla, CA). The cDNA isolated by RNA display (G1) was used as a probe to screen library filters containing 10⁶ plaques. Four positive clones were sequenced automatically through a sequencer (model 373; Applied Biosystems, Inc., Foster City, CA) and manually by dideoxy sequencing (Sequenase 2.0, USB, Cleveland, Ohio). Sequences were analyzed through the MacVector software (Oxford Molecular Group) and a contig was assembled through the Sequencher software (DNA Codes). The putative transcription initiation was mapped through the RACE protocol (Frohman et al., 1989). The resulting nucleotide and peptide sequences were aligned to databases of existing sequences through the BLAST network server (Altschul et al., 1990) and through a local Genetics Computer Group (GCG, Madison, WI) package (Devereux et al., 1984). Sequence searches were run against the GenBank, Swissprot, and dbEST databases.

Genetic Mapping

Genetic mapping was achieved using a ([C57BL/6j \times SPRET/Ei]F₁ \times SPRET/Ei) backcross (BSS) generated and distributed by The Jackson Laboratory (Bar Harbor, ME) (Rowe et al., 1994). A 596-bp G1.F/G1.A5 PCR fragment corresponding to the 5' of the *Eva* cDNA was used as a probe to identify a Taq1 restriction fragment length polymorphism (RFLP) by Southern hybridization. Its segregation was followed on 96 DNAs, corre-

sponding to the parents and 94 N₂ progeny, and then linkage analysis was performed with the MapManager 2.6 program (Manly and Elliott, 1991).

The human *Eva* orthologue was mapped in the human genome by Southern blot analysis on nine different YAC clones from the CEPH library (Albertsen et al., 1990) (735-C-9, 742-F-9, 785-C-6, 822-G-8, 828-G-11, 886-D-9, 901-A-11, 936-D-9, and 969-D-7). DNAs were digested with EcoRI and then hybridized with a radiolabeled *Eva* probe spanning the complete coding region. YAC clones were chosen based on synteny with the mouse mapping position.

RNase Protection Assay

An antisense riboprobe was generated by *in vitro* transcription of the G1 fragment subcloned into pBluescript with T3 RNA polymerase and incorporation of [α -³²P]UTP (800 Ci/mmol) (Promega Corp., Madison, WI). 50 μ g RNA from each of different adult mouse tissues were hybridized, treated, and then PAGE separated as described (Ausubel et al., 1995). A densitometer and the ImageQuant software (both from Molecular Dynamics, Inc., Sunnyvale, CA) were used for quantitative analysis of autoradiographs. Value normalization was achieved through a mouse β -actin riboprobe.

Reverse Transcriptase-PCR

B cells were isolated from a C57BL/6 spleen. After organ disruption, T cells were eliminated by complement-mediated cell lysis after incubation with anti-CD4, anti-CD8, and anti-Thy-1 mAbs (Coligan, et al., 1994). Then, B cells were positively selected with anti-B220 magnetic microbeads according to miniMACS cell sorting protocol (Miltenyi Biotec, Sunnyvale, CA). Mature T lymphocytes were positively selected with anti-Thy 1.2 magnetic microbeads from C57BL/6 mesenteric lymph nodes after B-cell depletion with anti-B220 magnetic microbeads. DN thymocytes were isolated from C57BL/6 thymi by positive selection with anti-CD25 mAb and goat anti-rat IgG magnetic microbeads. DP, single positive (SP) thymocytes, and macrophages were previously eliminated by complement-mediated lysis after incubation with anti-CD4, anti-CD8, and anti-macrophage mAbs. Macrophages were isolated from the peritoneal cavity (Coligan et al., 1994). Freshly drawn dendritic cells were obtained as described (provided by F. Galbiati, Hoffmann-La Roche, Milan, Italy) (Guery et al., 1996). Embryos at different days of gestation were separated from extraembryonic tissues under a dissection microscope. RNAs were isolated as described (Chomczynski and Sacchi, 1987). cDNA was generated from 1 μ g of RNA by using murine Moloney leukemia virus reverse transcriptase (RT) and oligo-dT (16 mer). G1-RT and G1-T3ON primer pair was used. The size of the amplified fragment on cDNA is 412 bp, whereas no amplified fragment is obtained from genomic DNA.

In Situ Hybridization

Mouse embryos of outbred CD-1 strain and thymi from RAG-2^{-/-} mice were embedded in paraffin, sectioned at 6 μ m, and then treated for *in situ* hybridization as described previously (Teesalu et al., 1996). The putative complete *Eva* coding sequence, subcloned into pBluescript II SK (Stratagene), termed *Eva.cds* was used to generate sense and antisense ³⁵S-labeled probes. After hybridization and washes, slides were dipped into Kodak NTB2 emulsion (Eastman-Kodak, Rochester, NY), exposed at 4°C for 1–3 wk and, after standard development, stained with toluidine blue and mounted in DPX mountant (BDH Chemicals Ltd., Dagenham, Essex, UK). Slides were observed and photographs were taken using an Axiophot microscope (Carl Zeiss, Inc., Thornwood, NY).

In Vitro Translation and Transfectants

The *Eva.cds* construct was used for *in vitro* transcription and translation experiments in the presence of [³⁵S]methionine, with or without microsomal membranes, as specified by the manufacturer (Promega Corp.). In some experiments, 10 μ l of translation mix were treated with the enzyme endo- β -N-acetyl-glucosaminidase H (endo-H) (Boehringer Mannheim Corp., Indianapolis, IN) as described (Ceriotti et al., 1995). Samples were analyzed by SDS-PAGE under reducing conditions and the resolved products were detected by fluorography.

A construct encoding the putative complete EVA protein tagged at the COOH terminus with a c-myc-derived epitope (Wong and Cleveland, 1990) was subcloned into pcDNA3 (Invitrogen, Carlsbad, CA) and introduced in monkey COS7 fibroblasts by DEAE-dextran-mediated transfection. 48 h after transfection, cells were trypsinized, plated on poly-L-lysine-coated glass coverslips (10⁵ cells), fixed with 3% paraformaldehyde, permeabi-

lized with 0.15% Triton X-100 in PBS for 5 min, and immunolabeled with 9E10 anti-myc mAb followed by FITC-conjugated F(ab')₂ fragments of goat anti-mouse IgG (Protos Immunoresearch, San Francisco, CA). Stable transfectants were obtained by introducing the same *Eva.myc* construct in CHO cells with the calcium-phosphate precipitation protocol and maintaining the cells in medium supplemented with G418 (600 μ g/ml).

Biochemical Analysis

A89A and TNC.R3.1 cells were washed three times with cold PBS, resuspended in ice-cold nuclease buffer (50 μ g/ml Staphylococcal nuclease, 2mM CaCl₂, 20 mM Tris-HCl, pH 8.8) for detachment with a cell scraper. The same nuclease buffer solution was used to harvest multiple plates to reach the final concentration of 50 \times 10⁶ cells/ml. The following antiproteases were added: 100 mM PMSF, 10 μ g/ml leupeptin, and 10 μ g/ml aprotinin; then 0.3% SDS and 10% β -mercaptoethanol were added and mixed on ice. Finally, 100 μ g/ml DNase I and 50 μ g/ml RNase A were added. Lysates were homogenized by passage through a 23-gauge syringe and were centrifuged in a microfuge for 10 min. COS7 and CHO transfectants were lysed in Triton X-100 lysis buffer (1% Triton X-100, 5 mM EDTA, 1 mM iodoacetamide, 1 mg/ml BSA, 10 mM Tris, pH 8.8, 0.15 M NaCl). Samples were subjected to SDS-PAGE under reducing conditions followed by transfer to nitrocellulose membranes and immunoblotted with 9E10 mAb and anti-EVA rabbit serum. Bound antibodies were revealed by peroxidase-conjugated goat anti-mouse (Dako Corp., Carpinteria, CA) or -rabbit (Sigma Chemical Co.) Ig sera, using the enhanced chemiluminescence detection system (Amersham Pharmacia Biotech, Inc., Piscataway, NJ).

Cell Fractionation

A89A and TNC.R3.1 cells were detached by incubation at 37°C for 10 min in 1 mM PBS-EDTA (10 ml for 50 ml of culture). After two washes in ice-cold PBS, cells were resuspended at 5 \times 10⁹/300 μ l in hypotonic buffer (20 mM Tris-HCl, pH 7.5, 1 mM EGTA, 1 mM MgCl₂, 0.5 mM DTT, and protease inhibitors) and incubated for 10 min on ice. Cells were then disrupted by homogenization on ice with a Dounce homogenizer (30 strokes at low speed and 10 strokes at maximum speed). Salt concentration was adjusted to 150 mM NaCl and intact cells, nuclei, and cytoskeleton were pelleted by centrifugation at 5,000 rpm for 5 min in a microfuge (Eppendorf Scientific Inc., Hamburg, Germany) at 4°C. After two washes in hypotonic buffer, the pellet (P1) was resuspended in Laemmli sample buffer. The low-speed supernatant was centrifuged at 100,000 g for 30 min and the resulting pellet (P100) was considered the membrane fraction, whereas the supernatant (S100) was considered the soluble proteins fraction. Equivalent amounts of all samples were resolved by SDS-PAGE in a 5–15% gradient gel and then immunoblotted with the indicated antibodies.

Cell Aggregation Assay

CHO cells, both pcDNA3- and *Eva.myc*-transfected, were detached by incubation at 37°C for 10 min in 1mM PBS-EDTA. After two washes in low-Ca Krebs-Ringer-Hepes (KRH) buffer (125 mM NaCl, 5 mM KCl, 1 mM MgSO₄, 1 mM KH₂PO₄, 0.1 mM CaCl₂, 33 mM glucose, 25 mM Hepes), cells were resuspended in low-Ca KRH-2% FCS (predialyzed against low-Ca KRH) to a final concentration of 2 \times 10⁶ cells/ml by three passages through an 18-gauge syringe. Single-cell suspensions were incubated in 2.5-ml polypropylene tubes with gentle rotation for 60 min at 37°C. Cells were finally plated on glass coverslips, treated, and then immunolabeled as described above. In similar experiments, cells were labeled with different fluorescent lipophilic dyes (Sigma Chemical Co.) before aggregation assay (Litvinov et al., 1994): either PKH2 (green fluorochrome) for *Eva.myc*-transfectants, or PKH26 (red fluorochrome) for vector-transfected CHO cells, were used. Aggregation index was calculated as $D = (N_0 - N_t)/N_0$, where N_0 is the initial number of particles corresponding to the total number of cells, and N_t is the number of remaining particles at the incubation time point t (Shimoyama et al., 1992).

Results

Identification and Cloning of *Eva*

To identify regulated genes during thymus development, we applied a modified RNA fingerprinting protocol (Mal-

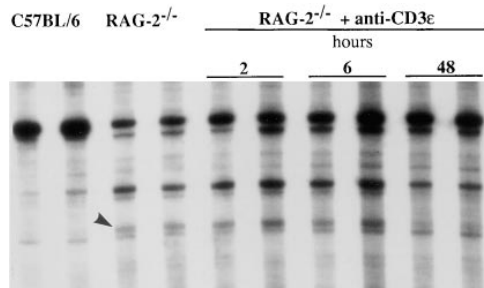


Figure 1. RNA fingerprinting experiment comparing cDNAs of thymi from C57BL/6, untreated RAG-2^{-/-} mice and RAG-2^{-/-} mice at different times (2, 6, and 48 h) after i.v. injection of anti-CD3ε mAb. RNA fingerprinting RT-PCR reactions were conducted in duplicate at each stage examined. *Arrowhead*; band corresponding to the *Eva* transcript.

garetti et al., 1997) to thymi from RAG-2^{-/-} mice at different intervals after the injection of anti-CD3ε mAb (2, 6, and 48 h). We identified a 436-nucleotide band (G1) that was selectively amplified in the thymus cDNA from untreated RAG-2^{-/-} mice. The same band was also detected in cDNA from RAG-2^{-/-} mice 2 and 6 h after treatment, but was almost absent at 48 h (Fig. 1). The band was gel-excised, reamplified, and then cloned into pBluescript II SK. Clones were screened as described (Consalez et al., 1996) and the plasmid G1.A2 was sequenced manually. A database search was run with BLASTN and BLASTX, using the GCG interface (Devereux et al., 1984). One mouse expressed sequence tag (EST) sequence (GenBank/EMBL/DBJ accession number AA288427), and several human ESTs (AA336903, H77296, W61215, H48606, AA088807, and N70439) displayed clear similarities to the G1 cDNA (from 99 to 84% identity). cDNA G1.A2 showed an open reading frame of 286 nucleotides, preceded by an in-frame stop codon. G1.A2 was used as a probe to screen a custom-made RAG-2^{-/-} thymus cDNA library. Sequence analysis and assembly of four positive clones revealed a

645-bp open reading frame encoding a deduced 215-amino acid (aa)-long sequence. Analysis of the predicted aa sequence with PROSITE, BLOCKS, and TMAP indicates that G1 encodes a type 1 transmembrane glycoprotein (Fig. 2 A), with a presumptive cleavable 20-aa-long signal peptide and a putative 25-aa-long transmembrane region (residues 151–175). Sequence comparison and alignments done with the PILEUP program showed a putative extracellular region containing a V-like domain: two cysteines (positions 47 and 123), corresponding to the invariant cysteines that form the intrachain disulfide bond in the Ig domain, are located 76 residues apart. The tryptophan at position 63, as well as other residues, such as glycine 40, arginine 90, leucine 109, and tyrosine 121 are typical features of V domains (Carayannopoulos and Capra, 1993). In addition, two potential glycosylation sites and a putative serine phosphorylation site were observed (Fig. 2, A and B). Based on database search results, we also sequenced the human cDNA clone containing H48606 EST, derived from a fetal liver/spleen expression library (I.M.A.G.E. clone N°202065). The human-derived sequence revealed the same features of G1 (Fig. 2 A), with an identity of 79 and 85% at the nucleotide and aa level, respectively. Moreover, database search results and sequence alignment revealed 33% identity and 45% homology with the myelin protein zero (Po), the predominant myelin protein in the peripheral nervous system (Fig. 2 C) (Lemke and Axel, 1985). The G1 nucleotide sequence did not match any known gene and protein (GenBank, EMBL, Swissprot, PIR), and thus represents a new gene, encoding a likely new member of the immunoglobulin superfamily. Based on the sequence and expression data (see below) we named this new gene *Eva*, for epithelial V-like antigen.

Chromosomal Localization of the Mouse and Human *Eva* Genes

A TaqI polymorphism was used to type the segregation of *Eva* alleles in the 94 individual N₂ progeny of the BSS

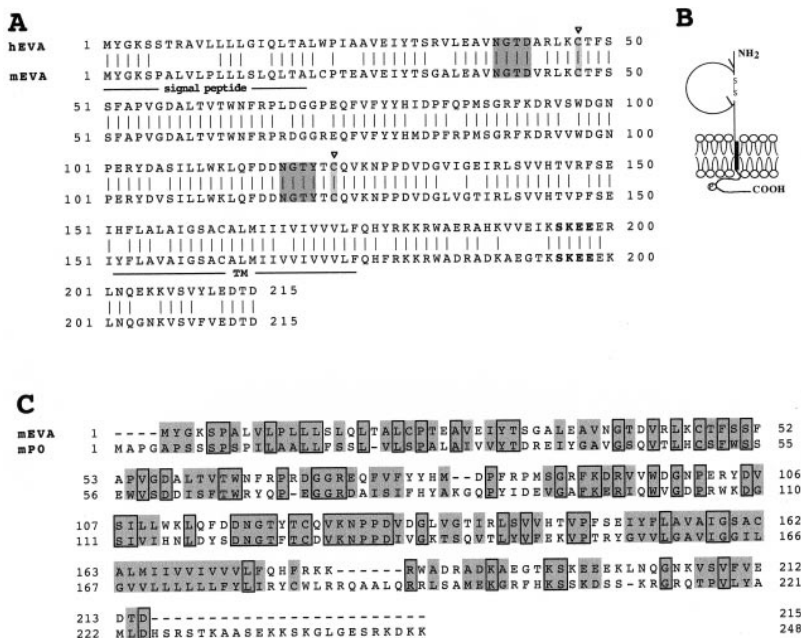


Figure 2. (A) Alignment of the aa sequences encoded by human and murine *Eva* cDNAs. *Left*, aa numbering. The predicted leader (signal peptide) and transmembrane sequences are labeled together with the following features: *dark-shaded boxes*, potential N-linked glycosylation sites; *light-shaded boxes*, cysteine residues (47 and 123) found in conserved positions within the V-type domain; *bold residues*, potential protein casein kinase 2 phosphorylation site. These sequence data are available under GenBank/EMBL/DBJ accession numbers AF030455 (for human *Eva*) and AF030454 (for mouse *Eva*). (B) Model of EVA protein according to prediction results. λ , N-linked glycosylation sites; P, putative protein CK2 phosphorylation site in the cytoplasmic tail. (C) Sequence alignment of mouse EVA and myelin Po proteins. Boxed residues are identical in the two proteins (33%); homologous residues are shaded (45%).

backcross by RFLP analysis. 90 out of 94 progeny were successfully typed. Linkage analysis unequivocally localized *Eva* to mouse chromosome (chr.) 9, 2.25 cM distal to *Xmv16* (LOD score 22.6), and 1.12 cM proximal to *Cyp1a2* (logarithm of the odds [LOD] score 24.4). The data are summarized in Fig. 3.

The human *Eva* orthologue was localized to chr. 11q24 by Southern blot analysis of YAC clones from the CEPH library. The YACs had been identified based on data bank information; in fact, some of the human ESTs homologous to *Eva* (namely H77296 and H48606, 84% identical to *Eva*) had been localized on chromosome 11q, between D11S1341 and D11S924, to the human genomic region syntenic to the mouse map position. DNA from nine YAC clones spanning that region were analyzed by Southern hybridization with a probe containing the complete *Eva* coding region. Of all YACs tested, *Eva* hybridizes YACs 822-G-8 and 828-G-11. YAC 828-G-11 has been mapped cytogenetically to 11q24 (Rocchi, M., see data available at http://bioserver.uniba.it/fish/rochi/webbari/2_YAC/800-899/828G11.html).

Regulated Expression of the *Eva* Gene in *RAG-2^{-/-}* Thymus

To confirm the expression data obtained by RNA finger-

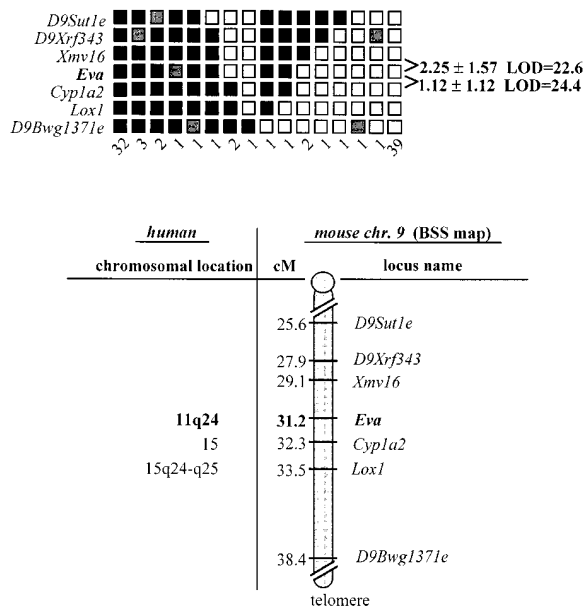


Figure 3. Mapping of *Eva* in the mouse genome. *Top:* haplotype and linkage analysis of *Eva* and flanking loci on mouse chromosome 9 through the analysis of the BSS backcross (The Jackson Laboratory). *Empty squares*, *Mus spretus* allele; *solid squares*, C57BL/6J allele; *stippled squares*, genotype not determined. Numbers to the right, between rows, indicate recombination fractions \pm standard error, and LOD scores. Columns represent different haplotypes observed on chromosome 9. Numbers below columns define the number of individuals sharing each haplotype. *Bottom:* position of *Eva* on chromosome 9 with respect to nearby markers independently mapped by others on the BSS backcross. Numbers on the left represent approximate genetic distances (cM) from the most centromeric chromosome 9 marker in this cross. Chromosomal locations of three syntenic human genes, including *EVA*, are also indicated.

printing, we performed Northern analysis on total RNAs extracted from thymi of C57BL/6 and *RAG-2^{-/-}* mice at different intervals after the injection of anti-CD3 ϵ mAb (2, 6, and 48 h). Hybridization was carried out with radiolabeled G1.A2 cDNA. As shown in Fig. 4 A, a 3.4-kb transcript in untreated *RAG-2^{-/-}* thymi as well as in *RAG-2^{-/-}* thymi at 2 and 6 h after injection was revealed. As predicted from the RNA fingerprinting pattern, no expression was detectable in wild-type and in *RAG-2^{-/-}* thymi 48 h after treatment. RNase protection assay (RPA) performed on the same samples (Fig. 4 B) revealed that *Eva* was also detectable in wild-type and *RAG-2^{-/-}* thymi 48 h after treatment upon a long gel exposure. Densitometric analysis after normalization with actin showed that *Eva* expression levels decrease at least 20-fold in *RAG-2^{-/-}* thymi 48 h after the treatment (data not shown). Furthermore, to confirm downregulation of the *Eva* transcript in this experimental model, we performed radioactive mRNA in situ hybridization experiments. The *RAG-2^{-/-}* thymus displayed a strong and uniform signal for the *Eva* transcript (Figs. 5 and 6), reminiscent of the embryonic thymus pattern (see below), whereas *RAG-2^{-/-}* thymus 48 h after injection failed to show any signal above background (Fig. 5, C and D); an analogous result was also obtained with wild-type thymus (data not shown).

Eva Distribution in Mouse Tissues and Cell Lines

Total RNA purified from adult mouse organs was used in

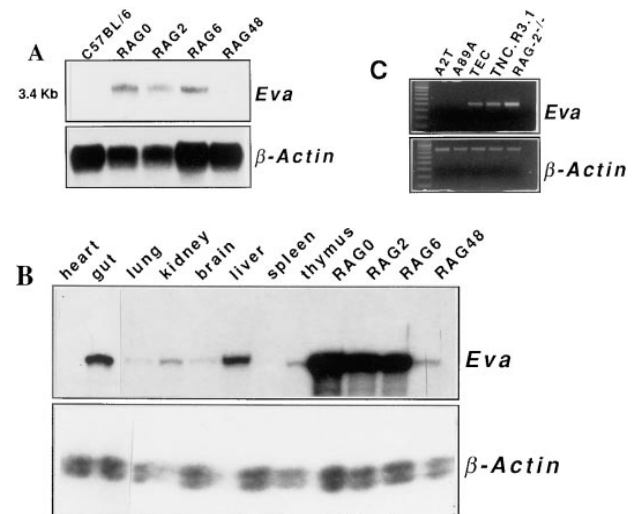


Figure 4. (A) *Eva* mRNA expression in wild-type and *RAG-2^{-/-}* thymi. Northern analysis on total RNA isolated from thymi of C57BL/6, untreated *RAG-2^{-/-}* mice and *RAG-2^{-/-}* mice at different times (2, 6, and 48 h) after anti-CD3 ϵ mAb injection. After hybridization with a labeled cDNA specific for *Eva*, the filter was stripped and again hybridized with a labeled β -actin probe. The apparent size of the transcript is indicated. (B) *Eva* mRNA expression in various adult mouse tissues. RNase protection assay with a 437-bp *Eva*-specific antisense riboprobe on seven adult mouse tissues and thymi of C57BL/6, untreated *RAG-2^{-/-}* mice, and *RAG-2^{-/-}* mice i.v. injected with anti-CD3 ϵ mAb. Results obtained with mouse β -actin riboprobe are also shown. (C) *Eva* mRNA expression in different thymic epithelial cell lines. RT-PCR on mRNA of four thymic epithelial cell lines (A2T, A89A, TEC, and TNC.R3.1). Gene expression on *RAG-2^{-/-}* thymus was used as control. cDNA-amplified fragment is 412-bp long.

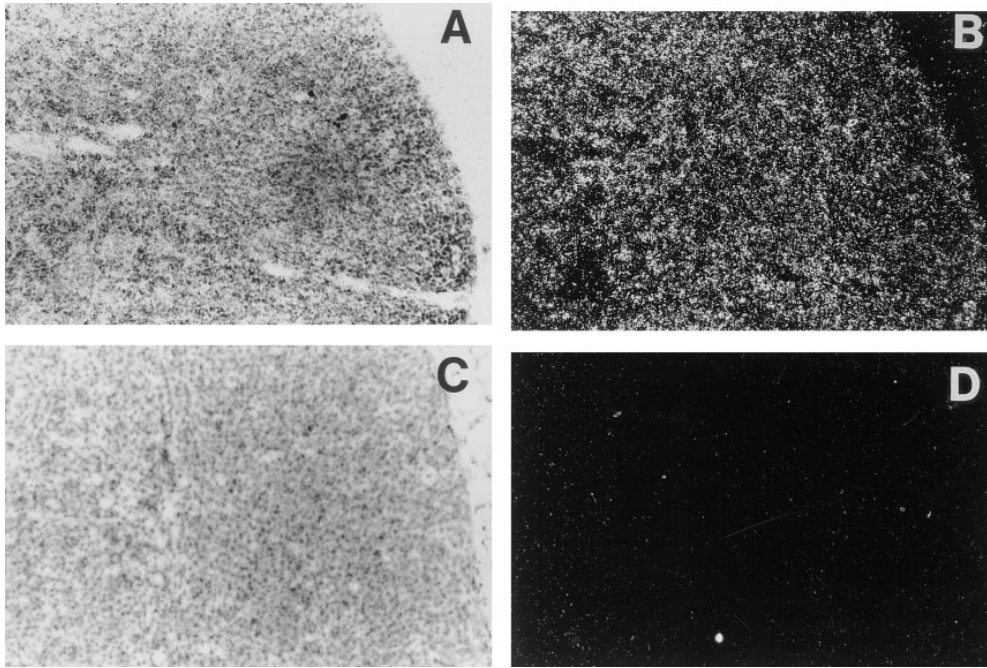


Figure 5. mRNA in situ hybridization of RAG-2^{-/-} thymi. *Eva* expression by RAG-2^{-/-} thymi from untreated mice (A and B) and treated animals at 48 h after injection of antibody (C and D). Bright-field views (A and C) and dark-field images (B and D). Note strong, homogeneous labeling of RAG-2^{-/-} thymus, and absence of *Eva* expression in the thymus from injected mice.

RPA to characterize the tissue distribution of the *Eva* transcript. As shown in Fig. 4 B, high expression levels of *Eva* were observed in the liver and gut, lower levels in the kidney, and very low ones in the lung and brain. No expression was observed by RPA in the spleen and heart. High levels of expression were also found in gut and liver from RAG-2^{-/-} mice (data not shown). *Eva* expression was also detected in the skin and testis by RT-PCR (Table I). Furthermore, we could detect the *Eva* transcript in wild-type fetal thymus and liver at day 13.5 post coitum (p.c.) and in whole embryos at the early primitive streak stage (day 7.5 p.c.) (Table I).

To assess the cellular specificity of the *Eva* transcript, we performed RT-PCR on purified cell populations. Table

I summarizes the results that define the non-T cell nature of the transcript. In fact, *Eva* was neither expressed in purified DN/CD25⁺ thymocytes that constitute the most abundant cell population in RAG-2^{-/-} thymus, nor in mature T cells. Similarly, no expression was observed in mature B lymphocytes, macrophages, dendritic cells, and bone marrow. To define the histological identity of *Eva*-expressing cells, we tested various cell lines by RT-PCR. No expression was observed either in MS-5, M210, and BMS2 cells (bone marrow stroma-derived), or in FDCP mix (representing multipotent hemopoietic precursor). Negative results on M15S, NIH3T3, MT2, and FSDC confirmed that *Eva* is not expressed in T lymphocytes, fibroblasts, macrophages, and dendritic cells. Interestingly, *Eva*

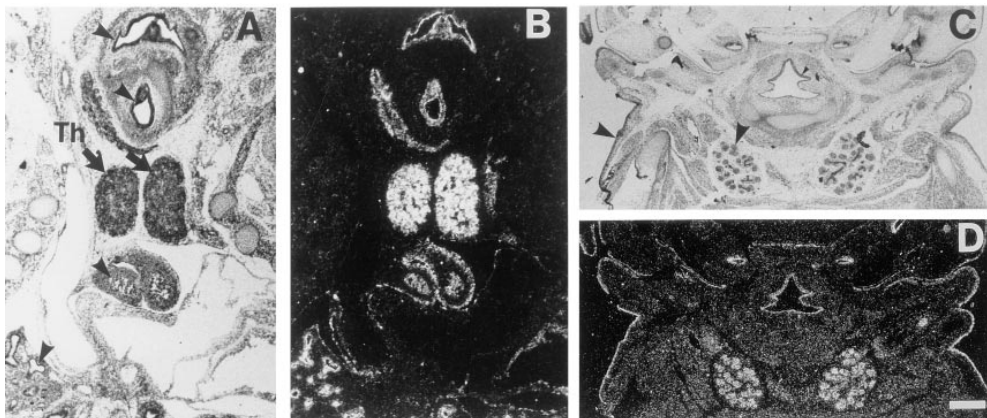


Figure 6. *Eva* mRNA in situ hybridization at 13.5 d.p.c. (A and B) and 14.5 d.p.c. (C and D) embryonic tissue sections. Bright-field images (A and C) and dark-field microphotographs (B and D). (A and B) High levels of *Eva* transcripts are found in the emerging thymus (A, arrows). Specific labeling can also be seen in epithelia lining the respiratory and gastrointestinal tracts: trachea, esophagus, gut and alveoli are indicated by arrowheads. (C and D) Note labeling of surface ectoderm and submandibular salivary glands (arrowheads). Bars: (A and B), 165 μ m; (C and D), 330 μ m.

Table I. Expression of *Eva* Assessed by RT-PCR

Ex vivo		Cell line	
Tissue			
Skin	+	T lymphocyte	
Testis	+	M15S	-
Cells		Macrophage	
CD25 ⁺ thymocyte	-	MT2	-
B lymphocyte	-	Dendritic	
T lymphocyte	-	FSDC	-
Macrophage	-	Fibroblast	
Dendritic	-	NIH3T3	-
Bone marrow	-	Bone marrow	
Fetal thymus		Stroma	
(day p.c.)		MS-5	-
13.5	+	M210	-
14.5	+	BMS2	-
16.5	+	Multipotent HSC	
Fetal liver		FDCP mix	-
(day p.c.)		Thymus	
13.5	+	Epithelium	
14.5	+	A89A	-
16.5	+	A2T	-
Embryo		TEC	+
(day p.c.)		MTE	+
7.5	+	24B6	+
8.5	+	TNC.R3.1	+
9.5	+	Thymocyte	
10.5	+	BW5147	-
11.5	+	M15T	-
11.5*	+	M14T	-
		Fibroblast	
		1D4	-

*Extraembryonic tissue.

transcript is clearly expressed in four (TEC, MTE, 24B6, and TNC.R3.1) out of six thymic epithelial cell lines (Table I and Fig. 4 C).

Localization of *Eva* Transcript during Mouse Development

We used radioactive *in situ* hybridization to localize *Eva* transcripts in mouse 8.5- and 9.5-d p.c. embryo implantation sites and in 12.5–16.5 d p.c. embryos. At 8.5-d p.c., abundant *Eva* expression was found in the extraembryonic ectoplacental cone and giant trophoblasts (Teeslau, T., manuscript in preparation), which are trophoectoderm-derived cells important for embryo implantation and placenta formation. In mouse embryos, *Eva* expression was found in a number of epithelial structures: surface ectoderm, and epithelia lining gastrointestinal and respiratory tracts as well as salivary glands (Fig. 6). At 13.5-d p.c., a prominent signal is evident in the developing thymus (Fig. 6, A and B), and persists through the later embryonic stages analyzed (data not shown).

Characterization of the *EVA* Protein

To validate sequence analysis data and assess the size of the peptide translated from *Eva* cDNA corresponding to the open reading frame, we performed *in vitro* transcription and translation, the latter in the presence or absence of microsomal membranes (Fig. 7 A). The translation product was subjected to SDS-PAGE analysis and two

peptide bands, the more abundant migrating with a molecular mass of 32 kD and a weaker one of 30 kD, were obtained only in the presence of microsomal membranes (Fig. 7 A, lane 6). Lack of protein product in Fig. 7 A, lane 5, at this exposure time, represented the transitional arrest by the excess of signal recognition particles described for secretory proteins in reticulocyte lysate system (Wolin and Walter, 1989). This observation suggested that *EVA* is a membrane-bound protein. The observed protein size was greater than the predicted one (24.5 kD), suggesting post-translational modifications of the peptide product. Consistently, treatment of the translated polypeptide with endo-H enzyme resulted in the appearance of two additional smaller bands of 30 and 24 kD, respectively, likely to be deglycosylation products (Fig. 7 A, lane 8).

To further substantiate *EVA* expression at the cell surface, a construct encoding *EVA* in frame with a COOH-terminal myc epitope tag (*Eva.myc*) was generated and transfected into cultured COS cells. A cellular immunofluorescence experiment run on permeabilized transfectants revealed that *EVA* is clearly present at the cell plasma membrane (Fig. 7 B).

An anti-myc immunoblot on Triton X-100 lysates of CHO cells transfected with the *Eva.myc* construct revealed a band with a molecular weight of 31–33 kD (Fig. 7 B). The predicted size of the recombinant protein is 25.7 kD, thus the difference between the predicted and the observed size (i.e., 6–8 kD) is in agreement with the one observed among the differently glycosylated products obtained in the *in vitro* translation experiments. Furthermore, both the recombinant proteins, *Eva.cds* and *Eva.myc*, were recognized in immunoblotting by a rabbit antiserum raised against an NH₂-terminal peptide of *EVA* (data not shown and Fig. 7 C). The same antiserum was tested in Western blot analysis on SDS lysates of TNC.R3.1 and A89A cells. Three bands with molecular weights of 32, 30, and 24 kD, respectively, likely corresponding to different glycoforms of *EVA*, were revealed in the TNC.R3.1 sample and were absent in A89A lysate. The same results were obtained under nonreducing conditions (data not shown), implying that *EVA* is expressed at the cell surface, and is devoid of interchain disulfide bridges.

Cell Separation and Homotypic Adhesiveness of *EVA*

The poor recovery of *EVA* in the soluble fraction of Triton X-100 cell lysates of thymic epithelial cell lines (data not shown) prompted us to separate cells into soluble and particulate fractions to determine the solubility of *EVA* and assess its association with the cytoskeleton, as it has been proposed for the Po protein (Wong and Filbin, 1994). TNC.R3.1 and A89A cells were lysed in hypotonic buffer and then separated in P1 (containing nuclei and cytoskeleton), P100 (membranes), and S100 (soluble proteins) fractions, as detailed in Materials and Methods. Immunoblots of these fractions with anti-*EVA* rabbit serum 833 revealed the almost exclusive presence of *EVA* in the P1 fraction of TNC.R3.1 cells at this exposure time (Fig. 7 D). Only long exposures of the membrane revealed the presence of *EVA* in the P100 fraction, implying that *EVA* is predominantly insoluble in hypotonic buffer. The same membranes were stripped and hybridized with anti-actin

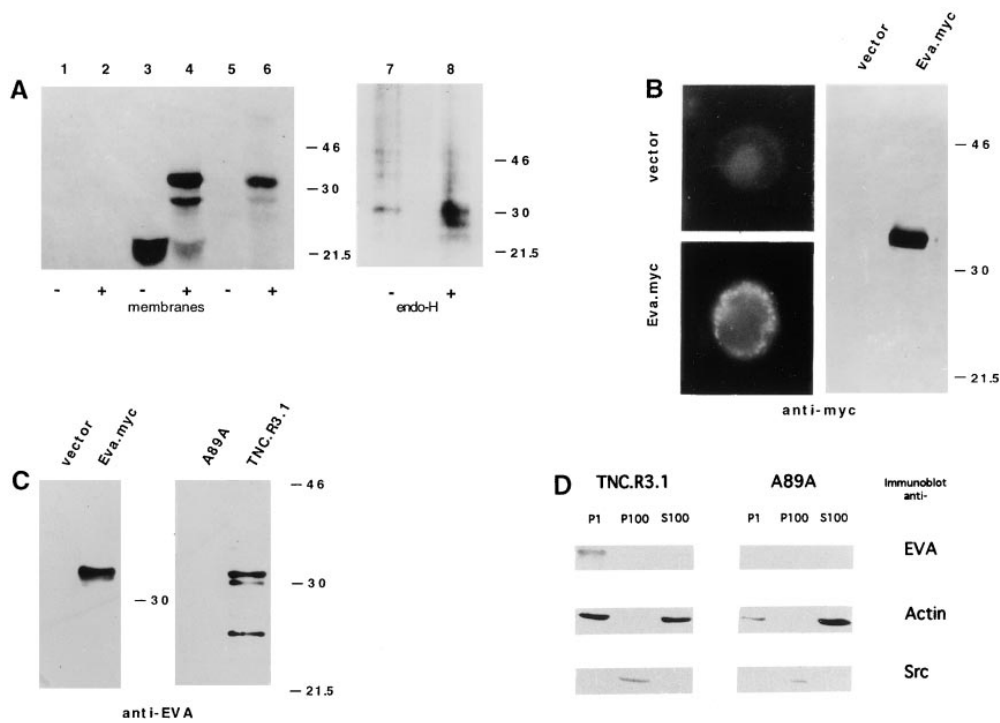


Figure 7. (A) In vitro translation of mouse *Eva* transcript. In vitro translation was performed in the absence (lanes 1, 3, and 5) or in the presence (lanes 2, 4, and 6) of canine pancreatic microsomal membranes. Translated polypeptides were fractionated through a 12% SDS-PAGE gel and then analyzed by fluorography. Lanes 1 and 2: no RNA as negative control. Lanes 3 and 4: *Saccharomyces cerevisiae* α -factor mRNA, used as positive control for both translation and glycosylation. The α -factor and the core-glycosylated precursor have molecular weights of 18.6 and 32 kD, respectively. Lanes 5 and 6, *Eva* mRNA. Lanes 7 and 8: *Eva* mRNA as in lane 6 or treated with the enzyme endo-H. Positions of molecular mass markers (in kDs) are indicated on the right.

(B) Cellular localization and immunoblot of chimeric EVA. *Left*, anti-myc immunofluorescence on CHO cells transfected with either pcDNA.3 vector (*top*) or *Eva.myc* vector (*bottom*). *Right*, anti-myc immunoblot on Triton X-100 lysates from the same cells. (C) Anti-EVA immunoblot. Western analysis with rabbit anti-EVA serum of Triton X-100 lysates from CHO cells transfected with either pcDNA.3 vector or *Eva.myc* vector and lysates in SDS of thymic epithelial cell lines A89A and TNC.R3.1. (D) EVA recovery in insoluble cell fraction. TNC.R3.1 and A89A cells were lysed in hypotonic buffer and separated into three fractions: P1, pellet of low-speed centrifugation; P100, pellet recovered after 100,000 g centrifugation, S100, soluble fraction. Equivalent amounts of all samples were resolved by SDS-PAGE in a 5–15% gradient gel and immunoblotted with rabbit anti-EVA antiserum, anti-actin and anti-src mAbs. EVA is exclusively present in the P1 fraction of TNC.R3.1 cells.

and anti-Src mouse mAbs. Fig. 7 D shows the presence of actin in the P1 and S100 fractions, as expected, and of Src exclusively in the P100 fraction, demonstrating the effectiveness of the lysis and the efficient isolation of cell membranes. The same result was obtained using TEC cells (data not shown). Whether the insolubility of EVA is due to formation of large homotypic aggregates (see below) or to association with cytoskeleton is under investigation.

To evaluate the adhesive properties of EVA-expressing cells, we performed an aggregation assay in which EVA.myc-transfected CHO and mock-transfected CHO cells were labeled with different lipophilic fluorochromes. Single-cell suspensions were allowed to aggregate and the presence of cell clusters was monitored by microscopic examination. As shown in Fig. 8 A, nonrecombinant pcDNA3-transfected CHO cells were scattered as a single-cell suspension, whereas EVA-expressing CHO cells formed large cell clusters after 60 min of incubation (Fig. 8 B). Large aggregates (> 10 cells) were observed only in the case of *Eva*-transfected cells and the aggregation index appeared to be fourfold higher than the one observed with parental cells (Fig. 8 C). Same results were obtained also when the aggregation assay was performed with unlabeled cells (data not shown). When monocellular suspensions of the two cell lines were mixed in a 1:1 ratio, EVA-expressing cells aggregated on their own (Fig. 8 D) in a 90-min assay, but not at 30 min, and random incorporation of parental

CHO into aggregates was observed within a range between 10 and 20% (data not shown). Furthermore, when the two unlabeled cell lines were mixed at a 1:1 ratio and stained with FITC-labeled 9E10 anti-myc mAb, the obtained cell clusters were selectively fluorescent, whereas scattered cells were detected only by phase-contrast analysis (Fig. 8, E and F). These results demonstrate that EVA expression can mediate cell aggregation, most likely through an homotypic interaction.

Discussion

Recombinase-deficient mice display a T cell maturation arrest at an early lymphoid precursor stage (DN CD25⁺ CD44⁻) (Shinkai et al., 1992). Since organogenesis depends on thymocyte–stroma cross-talk, this thymocyte defect also has an impact on the stromal component of the thymus, which fails to develop a medullary compartment (Holländer et al., 1995). Moreover, it is clear from various experimental systems that thymocytes at different maturation stages exert a distinct influence on stromal epithelial cells (Boyd et al., 1993; Ritter and Boyd, 1993). In RAG-2^{-/-} mice, massive transition to the thymocyte DP stage can be induced by in vivo cross-linking of CD3, which is expressed at low level on the membrane of RAG-2^{-/-} thymocytes (Jacobs et al., 1994; Shinkai and Alt, 1994). This treatment induces the characteristic phenotypic modifica-

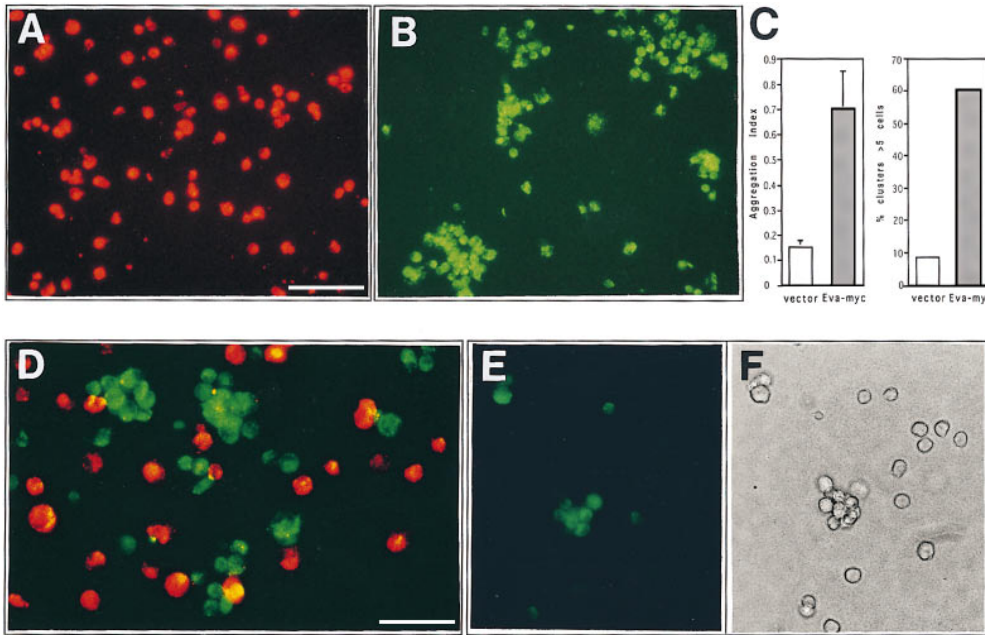


Figure 8. EVA-mediated cell aggregation. Nonrecombinant pcDNA.3-transfected CHO and Eva.myc-transfected CHO were detached and labeled, either with PKH26 or PKH2, respectively. After dissociation, the two cell lines were allowed to aggregate in suspension culture, either alone or mixed in a 1:1 ratio, and then analyzed 90 min after incubation in low Ca buffer. Vector-transfected cells are scattered as a single cell suspension (A), whereas large cell clusters are formed by Eva.myc-expressing cells (B). Extent of aggregation is expressed by aggregation index, calculated as $D = (N_0 - N_{90})/N_0$. Large aggregates (>5 cells) represented the 8.5% of the total events in mock-trans-

fected cells and 60% in Eva-myc cells (C). In the coculture, EVA-expressing cells aggregate on their own; random incorporation of parental CHO into aggregates never exceeded 10–20% (D). Coaggregation experiments with unlabeled cells were done as described above. Immunofluorescence staining with anti-myc mAb shows selective labeling of cells forming aggregates (E), when compared with phase-contrast analysis of the same field (F). Bars: (A and B) 50 μm ; (D–F) 25 μm .

tions occurring in thymocytes during the physiological transition (Nikolic-Zugic, 1991) and determines the expansion of the cortex that becomes histologically indistinguishable from the wild-type counterpart (data not shown).

We have exploited the possibility to time a synchronous T cell maturation event offered by this experimental system, with the aim of identifying regulated genes in the course of thymus development. RNA fingerprinting at different intervals after the injection of anti-CD3 ϵ mAb allowed us to isolate a new member of the immunoglobulin gene superfamily named *Eva*, whose expression is markedly downregulated at 48 h after the treatment, when thymocytes have completely downregulated the IL-2 receptor (CD25) and are in the CD4-8^{lo} stage, immediately preceding the acquisition of the DP phenotype. EVA is expressed in the epithelial component of the organ, thus is apparently downregulated by a signal, or extinction of a signal, coming from maturing thymocytes. Considering cytokines as potential inducers of EVA expression in the thymus epithelium, it is interesting to note that acquisition of DP phenotype, which constitutes the bulk population in wild-type thymus, is accompanied by the loss of cytokines' production (Zlotnik and Moore, 1995). This phenomenon was also observed in RAG-2^{-/-} mice for IFN γ and TNF α 48 h after anti-CD3 injection (our unpublished observations).

EVA bears a characteristic V-type domain and two potential N-glycosylation sites in the extracellular domain; a putative serine phosphorylation site for casein kinase 2 is also present in the cytoplasmic tail; those sites could account for posttranslational modification of the molecule. It shows a high degree of homology (45%) with the myelin Po protein, which is critically involved in compaction of

peripheral nervous system myelin via interactions through both its extracellular and cytoplasmic domains (Lemke and Axel, 1985). It has been shown that the immunoglobulin-like domain of Po mediates homophilic interactions of the molecule (Filbin et al., 1990); moreover, it has been proposed that the association of the cytoplasmic tail of Po with the cytoskeleton strengthens the homophilic adhesive interaction by inducing conformational changes and clustering of the extracellular domain (Wong and Filbin, 1996). The reported homology between Po and EVA prompted us to investigate functional similarities between the two molecules. Analogous to that observed with Po, we could show that EVA is largely insoluble in thymus-derived epithelial cell lines and that, after transfection of CHO cells, is able to mediate homophilic cell–cell adhesion.

In the thymus, the importance of epithelial interactions for appropriate organ histogenesis has been recently underlined by a study describing the absence of thymus organogenesis *in vitro*, in a reaggregated organ culture system, by blocking a homophilic interaction of E-cadherin (Muller et al., 1997). Various other cell adhesion molecules have been hypothesized to play a role in thymus morphogenesis (Patel and Haynes, 1993); the structural and functional properties of EVA are particularly attractive in this respect, offering a likely new candidate for such a role. The strong downregulation of *Eva* expression induced by thymocyte maturation and expansion might suggest a role for EVA in compaction of the thymic epithelial framework during early thymus organogenesis, a situation that is aberrantly procrastinated in RAG-deficient mice. The EVA-dependent adhesiveness of epithelium would not be needed once the thymocyte compartment has sufficiently

expanded. Suggestively, in the embryonic thymus, we could detect the highest level of *Eva* expression at 14-d p.c., which can be considered a developmental stage analogous to the one at which RAG-2^{-/-} mice are arrested, immediately preceding the expression of a rearranged TCRβ chain.

At present, we cannot rule out the possibility that EVA binds through a lectin-like interaction, as hypothesized for Po (Filbin and Tennekoon, 1991) and/or with an heterophilic ligand expressed on thymocyte, as it has been shown for E-cadherin (Karecla et al., 1995). If this were the case, EVA downregulation by DP transition would reflect the need of thymocytes to move to a more appropriate stage-specific niche in the organ. Accordingly, it has been shown that the progress of thymocyte maturation renders the cells less adhesive to stroma (Nishimura et al., 1990).

Finally, *Eva* expression in several epithelia suggests other potential roles for EVA in addition to the putative ones envisaged during thymus organogenesis. The early expression of *Eva* during embryogenesis and its selective epithelial localizations are particularly significant in this respect.

We thank A. Kruisbeck (Netherlands Cancer Institute, Amsterdam, The Netherlands) and P. Castagnoli (University of Milan, Milan, Italy) for cell lines; E. Barbier (Pateur Institute, Paris, France) for skillful advice in biochemistry; C. Sala (San Raffaele Scientific Institute) for YAC clones; K. Servis (University of Lausanne, Lausanne, Switzerland), P. Cordioli (Istituto Zooprofilattico, Brescia, Italy), S. Fabbri, S. Levi (both from San Raffaele Scientific Institute), P. Panina (Hoffmann-LaRoche, Milan, Italy), and A. Ceriotti (Consiglio Nazionale delle Ricerche, Milan) for reagents and experimental advice; and L. Adorini (Hoffmann-LaRoche, Milan), F. Blasi (University of Milan), and R. Pardi (San Raffaele Scientific Institute) for critically reading the manuscript. We are especially grateful to A.G. Siccardi (University of Milan) for constant support and encouragement.

Received for publication 23 December 1997 and in revised form 30 March 1998.

References

Albertsen, H.M., H. Abderrahim, H.M. Cann, J. Dausset, D. Le Paslier, and D. Cohen. 1990. Construction and characterization of a yeast artificial chromosome library containing seven haploid human genome equivalents. *Proc. Natl. Acad. Sci. USA*. 87:4256–4260.

Altschul, S., W. Gish, W. Miller, E. Myers, and D. Lipman. 1990. Basic local alignment search tool. *J. Mol. Biol.* 215:403–410.

Auerbach, R. 1960. Morphogenetic interactions in the development of the mouse thymus gland. *Dev. Biol.* 2:271–285.

Austyn, J.M., and S. Gordon. 1981. F4/80, a monoclonal antibody directed specifically against the mouse macrophage. *Eur. J. Immunol.* 11:805–815.

Ausubel, F.M., R. Brent, R.E. Kingston, D.D. Moore, J.A. Smith, and K.R. Struhl. 1995. *Current Protocols in Molecular Biology*. John Wiley and Sons, New York.

Boyd, R.L., C.L. Tucek, D.I. Godfrey, D.J. Izon, T.J. Wilson, N.J. Davidson, A.G. Bean, H.M. Ladyman, M.A. Ritter, and P. Hugo. 1993. The thymic microenvironment. *Immunol. Today*. 14:445–459.

Carayannopoulos, L., and J.D. Capra. 1993. Immunoglobulins. Structure and function. In *Fundamental Immunology*, 3rd edition. W.E. Paul, editor. Raven Press, New York. 283–314.

Ceriotti, A., E. Pedrazzini, M. De Silvestris, and A. Vitale. 1995. Import into the endoplasmic reticulum. *Methods Cell Biol.* 50:295–308. San Diego Academic Press.

Chang, A.C., S. Wadsworth, and J.E. Coligan. 1993. Expression of merosin in the thymus and its interaction with thymocytes. *J. Immunol.* 151:1789–1801.

Chomczynski, P., and N. Sacchi. 1987. Single-step method of RNA isolation by acid guanidinium thiocyanate-phenol-chloroform extraction. *Anal. Biochem.* 162:156–159.

Coligan, J.E., A.M. Kruisbeck, D.H. Margulies, E.M. Shevach, and W. Strober. 1994. *Current Protocols in Immunology*. E.R. Coico, editor. John Wiley and Sons, New York. 3.1.2–3.4.2.

Consalez, G.G., A. Corradi, S. Ciarmatori, M. Bossolasco, N. Margaretti, and

C.L. Stayton. 1996. A new method to screen clones from differential display experiments prior to RNA studies. *Trends Genet.* 12:455–456.

Corradi, A., L. Croci, C.L. Stayton, M. Gulisano, E. Boncinelli, and G.G. Consalez. 1996. cDNA sequence, map, and expression of the murine homolog of GTBP, a DNA mismatch repair gene. *Genomics*. 36:288–295.

Devereux, J., P. Haerberli, and O. Smithies. 1984. A comprehensive set of sequence analysis programs for the VAX. *Nucleic Acids Res.* 12:387–395.

Filbin, M., F.S. Walsh, B.D. Trapp, J.A. Pizze, and G.I. Tennekoon. 1990. Role of myelin Po protein as a homophilic adhesion molecule. *Nature*. 344:871–872.

Filbin, M.T., and G.I. Tennekoon. 1991. The role of complex carbohydrates in adhesion of the myelin protein Po. *Neuron*. 7:845–855.

Fine, J.S., and A.M. Kruisbeck. 1991. The role of LFA-1/ICAM-1 interactions during murine T lymphocyte development. *J. Immunol.* 147:2852–2859.

Frohman, M.A., T.R. Downs, P. Chomczynski, and L.A. Frohman. 1989. Cloning and characterization of mouse growth hormone-releasing hormone (GRH) complementary DNA: Increased GRH messenger RNA levels in the growth hormone-deficient lit/lit mouse. *Mol. Endocrinol.* 3:1529–1536.

Girolomoni, G., M.B. Lutz, S. Pastore, C.U. Assmann, A. Cavani, and P. Ricciardi-Castagnoli. 1995. Establishment of a cell line with features of early dendritic cell precursors from fetal mouse skin. *Eur. J. Immunol.* 25:2163–2169.

Glimcher, L.H., A.M. Kruisbeck, W.E. Paul, and I. Green. 1983. Functional activity of a transformed thymic epithelial cell line. *J. Immunol.* 171:1–11.

Gluzman, Y. 1981. SV40-transformed simian cells support the replication of early SV40 mutants. *Cell*. 23:175–182.

Godfrey, D.I., and A. Zlotnik. 1993. Control points in early T-cell development. *Immunol. Today*. 14:547–553.

Guery, J.C., F. Ria, and L. Adorini. 1996. Dendritic cells but not B cells present antigen complexes to class II-restricted T cells after administration of protein in adjuvant. *J. Exp. Med.* 183:751–757.

Hiai, H., Y. Nishi, H. Kaneshima, Y.O. Buma, and Y. Nishizuka. 1985. Thymic lymphoid-stromal cell complexes in mice: In vitro assay and mechanism of the complex formation. *Exp. Hematol.* 13:215–220.

Holländer, G.A., B. Wang, A. Nichogiannopoulou, P.P. Platenburg, W. van Ewijk, S.J. Burakoff, J.C. Gutierrez-Ramos, and C. Terhorst. 1995. Developmental control point in induction of thymic cortex regulated by a subpopulation of prothymocytes. *Nature*. 373:350–353.

Hueber, A.O., M. Pierres, and H.T. He. 1992. Sulfated glycans directly interact with mouse Thy-1 and negatively regulate Thy-1-mediated adhesion of thymocytes to thymic epithelial cells. *J. Immunol.* 148:3692–3699.

Hyman, R., and V. Stallings. 1974. Complement patterns of Thy-1 variants and evidence that antigen loss variants “pre-exist” in the parental population. *J. Natl. Cancer Inst.* 52:429–436.

Itoh, K., H. Tezuka, H. Sakoda, M. Konno, K. Nagata, T. Uchiyama, H. Uchino, and K.J. Mori. 1989. Reproducible establishment of hemopoietic supportive stromal cell lines from murine bone marrow. *Exp. Hematol.* 17:145–153.

Izon, D.J., L.A. Jones, E.E. Eynon, and A.M. Kruisbeck. 1994. A molecule expressed on accessory cells, activated T cells, and thymic epithelium is a marker and promoter of T cell activation. *J. Immunol.* 153:2939–2950.

Jacobs, H., D. Vandeputte, L. Tolcamp, E. de Vries, J. Borst, and A. Berns. 1994. CD3 components at the surface of pro-T cells can mediate pre-T cell selection in vivo. *Eur. J. Immunol.* 24:934–939.

Karecla, P.I., S.J. Bowden, S.J. Green, and P.J. Kilshaw. 1995. Recognition of E-cadherin on epithelial cells by the mucosal T cell integrin αM290β7 (αEβ7). *Eur. J. Immunol.* 25:852–856.

Lemke, G., and R. Axel. 1985. Isolation and sequence of a cDNA encoding the major structural protein of peripheral myelin. *Cell*. 40:501–508.

Leo, O., M. Foo, D.H. Sachs, L.E. Samelson, and J.A. Bluestone. 1987. Identification of a monoclonal antibody specific for a murine T3 polypeptide. *Proc. Natl. Acad. Sci. USA*. 84:1374–1378.

Lepesant, H., H. Reggio, M. Pierres, and P. Naquet. 1990. Mouse thymic epithelial cell lines interact with and select a CD31^{low}CD4⁺CD8⁺ thymocyte subset through an LFA-1-dependent adhesion-de-adhesion mechanism. *Int. Immunol.* 2:1021–1032.

Litvinov, S.V., M.P. Velders, H.A.M. Bakker, G.J. Fleuren, and S.O. Warnaar. 1994. Ep-CAM: A human epithelial antigen is a homophilic cell-cell adhesion molecule. *J. Cell Biol.* 125:437–446.

Lutz, M.B., F. Granucci, C. Winzler, G. Marconi, P. Paglia, M. Foti, C.U. Assmann, L. Cairns, M. Rescigno, and P. Ricciardi-Castagnoli. 1994. Retroviral immortalization of phagocytic and dendritic cell clones as a tool to investigate functional heterogeneity. *J. Immunol. Meth.* 174:269–279.

Margaretti, N., O. Pozzoli, A. Bosetti, A. Corradi, S. Ciarmatori, M. Panigada, M.E. Bianchi, S. Martinez, and G.G. Consalez. 1997. *Mmoil*, a new helix-loop-helix transcription factor gene displaying a sharp expression boundary in the embryonic mouse brain. *J. Biol. Chem.* 272:17632–17639.

Manly, K.F., and R.W. Elliott. 1991. RI Manager, a microcomputer program for analysis of data from recombinant inbred strains. *Mamm. Genome*. 1:123–126.

Muller, K.M., C.J. Luedeker, M.C. Udey, and A.G. Farr. 1997. Involvement of E-cadherin in thymus organogenesis and thymocyte maturation. *Immunity*. 6:257–264.

Negishi, I., N. Motoyama, K. Nakayama, S. Senju, S. Hatakeyama, Q. Zhang, A.C. Chan, and D.Y. Loh. 1995. Essential role for ZAP-70 in both positive and negative selection of thymocytes. *Nature*. 376:435–438.

Nikolic-Zugic, J. 1991. Phenotypic and functional stages in the intrathymic de-

- velopment of $\alpha\beta$ T cells. *Immunol. Today*. 12:65–70.
- Nishimura, T., Y. Takeuchi, Y. Ichimura, X.H. Gao, A. Akatsuka, N. Tamaoki, H. Yagita, K. Okumura, and S. Habu. 1990. Thymic stromal cell clone with nursing activity supports the growth and differentiation of murine CD4⁺CD8⁺ thymocytes in vitro. *J. Immunol.* 145:4012–4017.
- Patel, D.D., and B.F. Haynes. 1993. Cell adhesion molecules involved in intrathymic T cell development. *Sem. Immunol.* 5:283–292.
- Petrie, T., F. Livak, D.G. Schatz, A. Strasser, I.N. Crispe, and K. Shortman. 1993. Multiple rearrangements in T cell receptor α chain genes maximize the production of useful thymocytes. *J. Exp. Med.* 178:615–622.
- Pietrangeli, C.E., S. Hayashi, and P.W. Kincade. 1988. Stromal cell lines which support lymphocyte growth: Characterization, sensitivity to radiation and responsiveness to growth factors. *Eur. J. Immunol.* 18:863–872.
- Primi, D., B. Clynes, E. Jouvin-Marche, J.P. Marolleau, E., Barbier, P.A. Cazenave, and K. B. Marcu. 1988. Rearrangement and expression of T cell receptor and immunoglobulin loci in immortalized CD4⁺CD8⁺ T cell lines. *Eur. J. Immunol.* 18:1101–1109.
- Ritter, M., and R.L. Boyd. 1993. Development in the thymus: It takes two to tango. *Immunol. Today*. 14:462–469.
- Rowe, L.B., J.H. Nadeau, R. Turner, W.N. Frankel, V.A. Letts, J.T. Eppig, M.S. Ko, S.J. Thurston, and E.H. Birkenmeier. 1994. Maps from two interspecific backcross DNA panels available as a community genetic mapping resource. *Mamm. Genome*. 5:253–274.
- Sambrook, J., E.F. Fritsch, and T. Maniatis. 1989. *Molecular Cloning: A Laboratory Manual*. C. Nolan, editor. Cold Spring Harbor Laboratory Press, Cold Spring Harbor, NY. 545 pp.
- Sawada, M., J. Nagamine, K. Takeda, K. Utsumi, A. Kosugi, Y. Tatsumi, T. Hamaoka, K. Miyake, K. Nakajima, T. Watanabe, et al. 1992. Expression of VLA-4 on thymocytes. Maturation stage-associated transition and its correlation with their capacity to adhere to thymic stromal cells. *J. Immunol.* 149:3517–3524.
- Shinkai, Y., and F.W. Alt. 1994. CD3 ϵ -mediated signals rescue the development of CD4⁺CD8⁺ thymocytes in RAG-2^{-/-} mice in the absence of TCR β chain expression. *Int. Immunol.* 6:995–1001.
- Shinkai, Y., G. Rathbun, K.P. Lam, E.M. Oltz, V. Stewart, M. Mendelshon, J. Charron, M. Datta, F. Young, A.M. Stall, and F.W. Alt. 1992. RAG-2-deficient mice lack mature lymphocytes owing to inability to initiate V(D)J rearrangement. *Cell*. 58:855–867.
- Shimoyama, Y., A. Nagafuchi, S. Fujita, M. Gotoh, M. Takeichi, S. Tsukita, and S. Hirohashi. 1992. Cadherin dysfunction in a human cancer cell line: possible involvement of loss of alpha-catenin expression in reduced cell-cell adhesiveness. *Cancer Res.* 52:5770–5774.
- Spooneer, E., C.M. Heyworth, A. Dunn, and T.M. Dexter. 1986. Self-renewal and differentiation of interleukin-3-dependent multipotent stem cells are modulated by stromal cells and serum factors. *Differentiation*. 31:111–118.
- Teesalu, T., F. Blasi, and D. Talarico. 1996. Embryo implantation in mouse: Fetomaternal coordination in the pattern of expression of uPA, uPAE, PAI-1 and alpha 2MR/LRP genes. *Mech. Develop.* 56:103–116.
- Utsumi, K., M. Sawada, S. Narumiya, J. Nagamine, T. Sakata, S. Iwagami, Y. Kita, H. Teraoka, H. Hirano, M. Ogata, et al. 1991. Adhesion of immature thymocytes to thymic stromal cells through fibronectin molecules and its significance for the induction of thymocyte differentiation. *Proc. Natl. Acad. Sci. USA*. 88:5685–5689.
- van Ewijk, W. 1991. T-cell differentiation is influenced by thymic microenvironments. *Annu. Rev. Immunol.* 9:591–615.
- von Boehmer, H. 1994. Positive selection of lymphocytes. *Cell*. 76:219–228.
- von Boehmer, H., and H.J. Fehling. 1997. Structure and function of the pre-T cell receptor. *Annu. Rev. Immunol.* 15:433–452.
- Wadsworth, S., M.J. Halvorson, and J.E. Coligan. 1992. Developmentally regulated expression of the $\beta 4$ integrin on immature mouse thymocytes. *J. Immunol.* 149:421–428.
- Welsh, J., N. Rampino, M. McClelland, and M. Perucho. 1995. Nucleic acid fingerprinting by PCR-based methods: applications to problems in aging and mutagenesis. *Mutant. Res.* 338:215–229.
- Wolin, S.L., and P. Walter. 1989. Signal recognition particle mediates a transient elongation arrest of preprolactin in reticulocyte lysate. *J. Cell Biol.* 109:2617–2622.
- Wong, M.H., and M. Filbin. 1994. The cytoplasmic domain of the myelin Po protein influences the adhesive interactions of its extracellular domain. *J. Cell. Biol.* 126:1089–1097.
- Wong, M.H., and M. Filbin. 1996. Dominant-negative effect on adhesion by myelin Po protein truncated in its cytoplasmic domain. *J. Cell. Biol.* 134:1531–1541.
- Wong, P.C., and D.W. Cleveland. 1990. Characterization of dominant and recessive assembly-defective mutations in mouse neurofilament NF-M. *J. Cell Biol.* 111:1987–2003.
- Yanagihara, K., T. Kajitani, K. Kamiya, and K. Yokoro. 1981. In vitro studies on the mechanism of leukemogenesis. I. Establishment and characterization of cell lines derived from the thymic epithelial reticulum cell of the mouse. *Leukemia Res.* 5:321–329.
- Zlotnik, A., and T.A. Moore. 1995. Cytokine production and requirements during T-cell development. *Curr. Opin. Immunol.* 7:206–213.